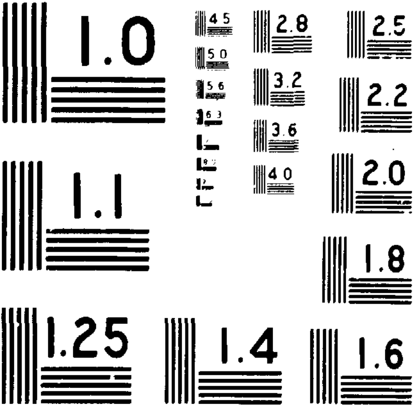

MICROCOPY RESOLUTION TEST CHART

NATIONAL BUREAU OF STANDARDS-1963

ZJE /99/ /1971/

M. BRUMOVSKÝ

INFLUENCE OF SOME METALLURGICAL VARIABLES ON THE RADIATION DAMAGE SENSITIVITY OF PRESSURE VESSEL STEELS

ŠKODA - Concern
NUCLEAR POWER PLANTS DIVISION, INFORMATION CENTRE PLZEŇ - Czechoslovakia

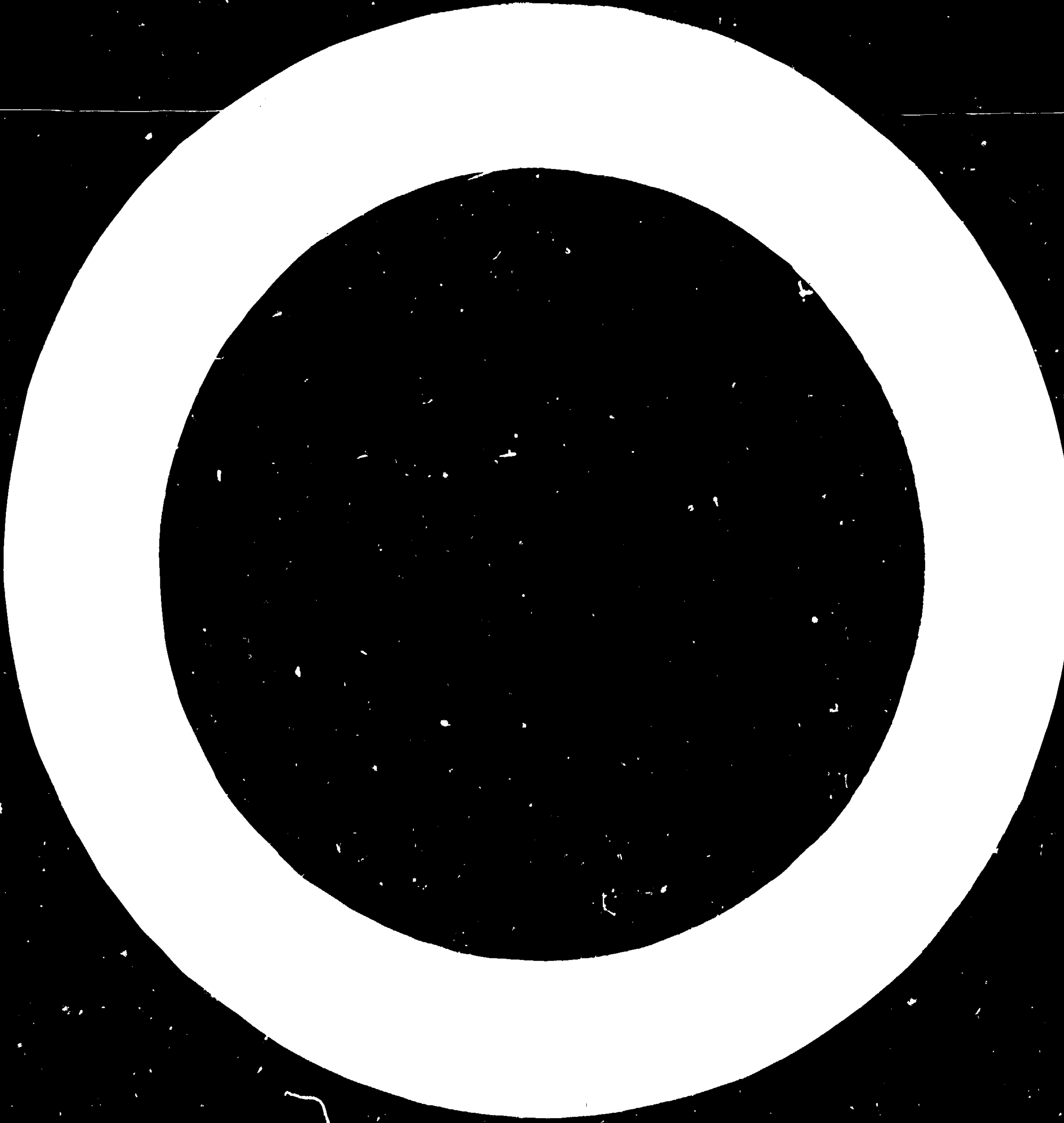

ZJE 99 1971

M. Brumovský

INFLUENCE OF SOME METALLURGICAL VARIABLES ON THE RADIATION DAMAGE SENSITIVITY OF PRESSURE VESSEL STEELS

Paper presented at the 5th International Symposium on the Effects of Radiation on Structural Materials held in Niagara Falls, Ontario, Canada, June 29 - July 1, 1970.

ŠKODA CONCERN
Nuclear Power Plants Division, Information Centre
PLZEŇ, CZECHOSLOVAKIA

ABSTRACT

Study of some binary and ternary alloys of Fe-C-Mn type were performed to understand the mechanism of radiation hardening and embrittlement in nuclear reactor low-carbon pressure vessel steels.

Results of static tensile tests showed the substantial effect of carbon and manganese contents. Carbon, resp. pearlite content in alloys, increases the resistance against radiation damage during irradiation at 80 to 100 deg C, while manganese content higher than 0.5 to 1.0 weight per cent decreases this resistance.

"Supersaturation" connected with the decrease of yield strength, was observed in iron and Fe-C type alloys at neutron doses higher than 5×10^{19} n/cm^2.

Influence of the initial yield strength value upon its increase during irradiation has been shown for low-carbon steel with various heat-treatment or various cold work value.

Printed by
Czechoslovak Atomic Energy Commission
Centre for Scientific and Technical Information
Zbraslav nad Vltavou

Introduction

Radiation damage in low-carbon pressure vessel steels has been intensively studied for more than last 15 years especially for their importance in safe operation of the whole nuclear power plant. By this time we have very comprehensive collection of various results of radiation damage in this type of steels, but only in last several years some partial studies of the explanation of damage mechanism, especially physical and mechanical property change and of the effect of steel structure and composition has been started.

This paper tries to explain some of the basic problems which substantially can influence the sensibility of low-carbon steels to the radiation damage. The study has been aimed to the isolation of the effect of carbon and manganese contents, first of all, as carbon and manganese are elements which determine mechanical properties and structure of this type of steels in significant manner. Mechanical properties of these alloys depend also on other variables; thus the study of the influence of initial stage of material were performed, too. For the first part of this study, Fe-C-Mn type alloys, as representative alloys for low-carbon steels, were used, while commercial steel for the A-1 reactor was used for the second part of the experimental program.

The results of this study can be divided into three sections: (1) effect of neutron dose and saturation effect, (2) effect of carbon and manganese contents, (3) role of initial stage of material. As the conclusion the model for radiation hardening in Fe-C-Mn type alloys is proposed.

Experimental details

Materials

Experimental binary and ternary Fe-C-Mn type alloys were prepared by double vacuum melting from carbonyl powder iron in the Institute of Iron Metallurgy in Prague. All heats were deoxidized by carbon and then alloyed by carbon and manganese to the required composition. Weight of ingots was approximately 3 kg. Specimens were machined from forged rods and then heat treated in vacuum at 900 C (1652 F) - 1 hr + 650 C (1202 F) - 1 hr with cooling in vacuum furnace. Chemical composition of all heats and their basic mechanical properties are summarized in Tab. 1 and 2. Solid solution nitrogen content was determined according to the results of Shozo et al / 1 / as 15 to 20 wt.ppm. Grain size in all heats is very similar in diameter, approximately ASTM 6 to 8 grade. Microstructure of alloys depends on chemical composition; some of alloys have pure ferritic structure (pure iron and Fe-Mn type alloys), other have ferrite - pearlitic type (Fe-C and Fe-C-Mn type alloys) and one alloy (XM) has almost eutectoidal one. Then the influence of carbon and manganese contents can be studied separately in binary alloys and similarly the combined effect of both elements in ternary alloys, first of all in "diagonal" of contents between 0 % (C + Mn) and 0.35 % C + 1.8 % Mn, as it is seen in Fig. 1.

Low carbon steels, used in second part of this research programme, were prepared by the same technology, as for the A-1 pressure vessel, i.e. as ČSN 13030.9 Ni, Al + Ti modified steel. Parent material and welding joints were studied; their chemical composition and initial mechanical properties are summarized in Tab. 3.

Mechanical Testing

Static tensile, microhardness and impact properties were measured. For static tension tests two types of specimens were used - specimens with diameter 1.2 mm for Instron tensile machine (strain rate $7\times10^{-5}\,sec^{-1}$) and with diameter 1 mm for MI 34 Chevenard type machine (strain rate $7\times10^{-4}\,sec^{-1}$), all tests were performed at 20 C (68 F). Stress-strain diagrams were evaluated with the use of digital computer to determine several parameters, first of all parameters of Petch law according to Cottrells / 2 / extrapolation method.

For impact tests, "hot cell" type specimens were used, with diameter 5 mm and 30 mm length with circumferential 1 mm deep V-notch with 60-deg angle and 0.25 mm bottom radius. Transition temperature increase has been determined from 3 kgm/cm^2 fracture toughness, which is very near to the 0.4 criterion.

Microhardness was measured by Hanemann method with 20 g load.

Irradiations

Irradiations were performed partially in the Institute of Nuclear Research in Řež near Prague in VVR-S reactor up to the dose $5.2\times10^{18}\ n/cm^2$ at temperatures 80 to 100 C (176 to 212 F) and partially in the Institute of Atomic Energy in Moscow in SM reactor up to the dose $5.1\times10^{19}\,n/cm^2$ at temperatures 160 to 180 C (320 to 356 F). All doses, mentioned in this paper, mean neutrons with energy higher than 1 MeV.

Effect of neutron dose and saturation effect

For iron and pressure vessel steels several relations for yield strength increase have been derived. As the simple relations with 1/2 or 1/3 root dependence are not valid in whole dose interval, Makin / 3 / proposed following expression, based on the idea that saturation effect might take place at higher irradiation doses :

$$\Delta\sigma_Y = A\left[1 - B.\exp(-C.\phi t)\right]^{1/2} \qquad (1)$$

where A, B, C are constants,

ϕt is neutron dose.

Blewitt / 4 / used improved calculations of de Wit / 5 / and Foreman / 6 / for the activation stress of Frank-Read source and found for the yield strength value of copper :

$$\sigma_Y = A(B_1 + B_2\cdot\phi t)^{1/2}\left[\ln\frac{(B_1+B_2\cdot\phi t)^{-1/2}}{b} + B\right] \qquad (2)$$

where A, B_1, B_2, B are constants,

b is Burgers vector.

This expression involves not only saturation effect but also effect of some "supersaturation". Last one is caused by the shortening of mean distance between zones below some critical value and must be expressed as "softening", i.e. by lowering of yield strength value. From equation (2) it is very difficult to determine some simple relation for yield strength increase, it is clear that the exact value of exponent must fall, as neutron dose is rised.

For b.c.c. metals, including our experimental iron alloys, according to the Johnson´s / 7 / interpretation of Petch law, we can suppose that above mentioned equation (2) is valid only for "friction" stress, σ_i. Only for high doses, higher than approximately 10^{19} n/cm^2, it is possible to use approximation as

$$\sigma_i \doteq \sigma_{LY} \tag{3}$$

as the second part of Petch law, i.e. $k_y d^{-1/2}$, is falling down to the zero; accuracy of this approximation is better than 10 %. Possibility of this approximation is illustrated in Fig. 2, where values for lower yield strength, σ_{LY}, friction stress, σ_i, and 5 % flow stress, σ_5, are sketched together.

The "saturation" dose is than given as

$$(\phi t)_{sat} = \frac{\exp\left[2\left(B-1-\ln b\right)\right] - B_1}{B_2} \tag{4}$$

and for pure iron, according to the experimental results, calculated value is 6×10^{19} n/cm^2, which is very close to experimental one, which has been found as 4×10^{19} n/cm^2. Both these values are in a good agreement with calculations of Beeler / 8 / or experiments of Bement / 9 / and McRickard / 10 /. Supposing the parameter B_2 characterizes the efficiency of neutron bombardment, i.e. number of zones, produced by one neutron in ccm, then parametr B_1 represents initial density of precipitates and other similar defects, determining yield strength value. Bryner / 11 / observed that B_2 for irradiated iron is equal to 5.6×10^{-5} which is approximately by three or four orders smaller, than theoretical value from simple hard sphere model

calculations. As the mean distance between two zones at saturation zone is equal to $(B_1 \ll B_2 \cdot \phi t_{sat})$:

$$L = 2\left\{3\left[4\pi B_2 (\phi t)_{sat}\right]^{-1}\right\}^{1/3}, \tag{4a}$$

then this distance for iron lies between 800 and 900 Å, which is at least ten times larger than the mean zone diameter.

Existence of the "supersaturation" is in the best way illustrated by Fe-C type alloys, as is seen in Fig. 3. Increase in carbon content causes the decrease of saturation dose and the more pronounced "softening" in supersaturation region. Process of softening, observed in yield strength changes, does not influence plasticity properties. Both elongations - homogenous and total - decreased with higher neutron doses as the higher concentration of zones (nonhomogenities in material) must cause smaller elongation in specimen. Higher content of pearlite in alloys causes larger yield strength decrease during supersaturation. This fact shows the dominating role of pearlite in this effect, as in pure iron similar sharp yield strength drop has not been observed. During irradiation not only ferrite, but pearlite is damaged too. Damage in ferrite causes its hardening and then slow softening in the supersaturation region. On the contrary, damage in pearlite (which is very hard and brittle phase in alloy and determines high initial yield strength value) can cause only the softening of this phase by the accelerated migration of point defects and carbon atoms, so that the phase boundaries (between ferrite and cementite) must change from sharp form to the diffusion type which results in yield strength decrease. In the same way at saturation dose the mean distance between zones (and other type of defects) is smaller than 1000 Å which is much less than the thickness of pearlite lamelias - this small distance and high concentration of defects must influence phase boundary sharpness.

For lower neutron doses ferrite is the dominant factor, which results in the increase of yield strength (or stress σ_i) value. For high doses, both effects take place together. At the highest doses, supersaturation in ferrite occurs slower, than in pearlite, so the last one has the dominating role in final result.

This combined effect of both phases is also confirmed by the microhardness changes, as is seen in Fig. 4. Microhardness of ferrite shows increasing tendency, at least up to the neutron dose of $5x10^{18}$ n/cm^2 (range of measurements) but microhardness of pearlite first goes through local minimum, caused probably by the migration of point defects (vacancies) to the phase boundaries, and then appears rapid tendency to saturation at the values, lower than initial ones.

Manganese, as substitute atom in solid solution, caused only alloy hardening in initial stage. During irradiation different affinity of manganese atoms to the nitrogen and carbon atoms / 12 / and point defects probably creates complexes of these manganese atoms with carbon or nitrogen atoms or point defects. This effect is pronounced only for manganese contents higher than approximately 0.3 wt. %, as for lower contents most of manganese atoms are not free (are joined to carbon or nitrogen atoms) and only excess manganese atoms are able to create above mentioned complexes, which substantially enlarge yield strength increase. This assumption is also based on the higher microhardness increase in manganese alloyed ferrite than in pure ferrite, which shows to the same additional process of hardening, dependent on manganese presence. As Fe-Mn type alloys are only one phase type (of ferritic structure), tendency to the saturation and oversaturation is very similar to the behaviour of pure iron; only some tendency to the increase of saturation dose for higher manganese content has been observed, as not all point defects and manganese atoms took place in the zone formation (because of some formation of complexes with manganese atoms), so their diameters are smaller and their efficiency in yield strength increase is lower.

In Fe-C-Mn type alloys both effects take place together, so alloys with higher carbon content and lower manganese content (XL) show saturation close to $5x10^{19}$ n/cm^2, other alloys, especially with higher manganese content, are not saturated up to this neutron dose and their calculated values are close or higher than $10^{20} n/cm^2$. This situation is similar to the irradiation effects in pressure vessel steels, for which the saturation dose has not yet been observed. It seems that all alloying elements, as Mn, Cr, Ni etc., or impurities, as P, S etc., increase the saturation dose to higher values, as the mechanism of radiation damage becomes more complex.

Effect of carbon and manganese content

Tensile properties

Results, discussed in previous chapter, have shown the substantial influence of carbon and manganese content on the radiation damage value in Fe-C-Mn type alloys, as it is seen in Fig. 5. For lower irradiation doses at 80 to 100 C, changes in friction stress, σ_i , are better representative for radiation damage mechanism than yield strength increase. Decreasing tendency of the friction stress change with increasing carbon content in iron alloys also shows to the fact that the most hardenable phase in this type of alloys is ferrite only and that pearlite cannot practically participate in radiation hardening. Proof of this assumption can be also seen in slopes value of curves for Fe-C type alloys; these slopes are almost independent on neutron dose. "Softening" role of pearlite at these neutron doses has not yet been pronounced, as the concentration of zones and defects is low in relation to the dimensions of pearlite lamellas. Friction stress increase is then directly proportional only to the ferrite content in alloy and to the neutron dose.

Manganese perceptibly influences friction stress increase in contents higher than approximately 0.5 wt.%, as for alloy Fe-0.3 Mn no positive effect of manganese has been observed. Independency on manganese content for the lowest dose can depend on the fact that manganese atoms are not yet active for complex creation, as the radiation induced damage is not yet so large to overnumber substantially the initial concentration of defects. The influence of manganese content is raised with the dose increase. If the manganese content is higher, the probability of complex creation (i.e. creation of complexes of manganese atoms with carbon, nitrogen atoms or point defects) is higher. These complexes cause large increase in yield strength or friction stress, due to their pinning of dislocations.

Fe-C-Mn type alloys are controlled by carbon content (i.e. by ferrite content) at lower doses; for higher doses the influence of manganese becomes more important. Both effects are additive and cause that the friction stress increase becomes nearly independent on carbon and manganese content for alloys, lying on our "diagonal" of contents in Fig. 1.

Alloy XO, with lower manganese content in comparison with diagonal alloys, has shown lower friction stress increase, as the carbon effect is higher than manganese one.

Higher irradiation temperatures (160 to 180 C) have caused very similar dependence, as it can be seen in Fig. 3 and better in Fig. 6. Maximum damage value in Fe-C type alloys can be observed at carbon content about 0.10-0.15 wt.%; yield strength increase is higher than for pure iron. Only at higher carbon contents the suppressing effect of carbon is expressed; this local maximum could be caused by the precipitation of metastable ε-carbides, as Damask et al. /13/ observed in iron at this temperature range. These carbides cause an extra hardening of ferrite, as it is observed especially in alloy XB. The effect of hardening by ε-carbides cannot be observable in pure iron, as there are not any sufficient sources of suitable carbon in pure ferrite (as, on the contrary, acts pearlite phase in Fe-C type alloys). For higher carbon content the ferrite content in alloy is lower, so lower is the ferrite hardening by ε-carbide precipitation, and lower is the yield strength increase in alloys, because pearlite is not effective in this process.

Behaviour of Fe-Mn type alloys is not different from that in lower irradiation temperatures, as only one phase - ferritic - alloys are present.

Radiation damage in Fe-C-Mn type alloys is influenced by manganese content, preferably, only for alloy XO yield strength increase is determined by low carbon content as simultaneously manganese content in alloy is relatively small. Different behaviour has been observed in yield strength increase in alloy XM, which is difficult to explain - but the microstructure of this alloy - large pearlitic blocks surrounded by chains of fine ferritic grains must play important role. As the ferrite content is small then in this case pearlitic phase must be hardened, too, probably by the precipitation of manganese carbides, similar to ε-carbides in iron.

Parameter k_y is decreasing with neutron dose increase, for all types of alloys. In Fe-C type alloys decrease of this parameter, as it is seen in Fig. 5, for doses up to $5x10^{18}$ n/cm^2 is approximately of the same order - into 0.8 to $1.0x10^7$ C.G.C. units, while for Fe-Mn type alloys this decrease is much sharper, especially for alloys with manganese content

higher than 1 wt. %; after the same dose parameter k_y has decreased to $0.1x10^7$ C.G.S. units. Fe-C-Mn type alloys also show decreasing tendency in k_y, similar to the superposition of both binary alloys. Large decrease of k_y to the low values demonstrate that the behaviour of grain and phase boundaries is influenced by irradiation, especially by the creation of complexes of manganese atoms with point defects and carbon or nitrogen atoms, as for Fe-Mn type alloys this decrease is the most strong one. Low values of k_y indicate full exhaustion of carbon and nitrogen atoms from solid solution (according to /14/) and manganese atoms this process accelerate.

Impact properties

For studied alloys, radiation embrittlement, as defined by transition temperature increase from impact notch tests, must be based on the similar mechanism, as radiation hardening. Specimens for these tests were irradiated only by one dose (at 80 to 100 C), so it has not been possible to study neutron dose effect.

Transition temperature increase in Fe-C type alloys, as is shown in Fig. 7., depends on the ferrite content by the same way, as for tensile properties. The decrease of ferrite content in alloy has caused suppresing of the sensitivity to the radiation embrittlement. Then ferrite must be, as in previous case, the most sensitive phase of alloy and is most embrittled by irradiation. Pearlite is much more brittle in the initial stage (which results in higher initial transition temperature value) than ferrite, thus radiation damage cannot cause any large changes in properties, as in ferrite is done.

Fe-Mn type alloys with manganese content higher than 1 wt.% have shown strong sensitivity to the radiation embrittlement which must be caused by the same reason, as for yield strength increase. Behaviour of Fe-C-Mn type alloys, lying in "diagonal" of contents, is very similar to each other; difference between individual alloys is very small (less than ± 5 C). These results are in a good agreement with several works with low carbon steels, for which transition temperature increase is practically independent on the chemical content and treatment of steel. Somew. t higher value for alloy XS is caused by higher manganese content in relation to the carbon content, but this value is not also very far from the other values.

Role of initial stage of material

In equation (2) parameter B_1 represents the initial concentration of all types of defects which can influence the friction stress value in alloys. Detailed calculations and comparison of the friction stress increase with the value of B_1 has not shown any strong dependence on this parameter for all types of alloys; much more important microstructure and type of alloy has been discovered. This effect of the initial stage takes place especially in the case when one type of alloy or steel (or group of very similar steels) is chosen and studied. Only in this event different initial concentration of defects, caused either by cold work or by heat and technological treatments, are dominant factors for radiation damage value.

Simplifying equation (2), first approximation can be written as

$$\sigma_i \doteq A(B_1+B_2\cdot\phi t)^{1/2} = A'(N_o+N_{ir})^{1/2} \qquad (5)$$

Then it can be shown for low irradiation doses the dominant role for friction stress value plays initial concentration of defects, N_o; for high neutron doses becomes more important concentration of radiation induced defects, N_{ir} . For small irradiation doses, if $B_1 > B_2.\phi t$, i.e. $N_o > N_{ir}$, it is possible to write (neglecting higher order terms)

$$\sigma_i \doteq A.N_o^{1/2}\left(1+\frac{1}{2}\frac{N_{ir}}{N_o}\right) \qquad (6)$$

which means that for friction or yield strength increase we can find

$$\Delta\sigma_i \doteq \Delta\sigma_{LY} \doteq A'\frac{N_{ir}}{N_o^{1/2}} \qquad (7)$$

As the friction stress value for small values of N_{ir} is proportional to the square root of initial concentration of defects, i.e. to $N_o^{1/2}$, then it is possible to rewrite the expression (7) as

$$\Delta\sigma_i \doteq \Delta\sigma_{LY} \doteq \bar{A}\,(\sigma_{LY})_o^{-1} \qquad (8)$$

which is valid for low neutron doses. For higher doses this dependence becomes more complicated and exponent is decreasing to the zero. Results, summarized in Fig. 8, illustrate well this situation. In part "a" several different heats and welding joints of ČSN 13030.9 Ni, Al + Ti steel were studied. For lower dose, 6.1×10^{18} n/cm^2, this exponent is near to one, for higher dose, 1×10^{19} n/cm^2, exponent n is decreasing to 0.6 with tendency to be independent on the initial yield strength value for very high doses. This effect means steel with higher initial yield strength value is hardened by irradiation in a smaller degree, than steel with lower initial yield strength.

Part "b" in the same figure represents the results from irradiated specimens of the same steel with different initial cold work value, i.e. with initial dislocation density. Similar results, as for the part "a", are shown; only changes in exponent are smaller as the neutron doses are lower. This situation can be illustrated by curves in Fig. 1, as the higher initial cold work value caused increase in initial yield strength value, but the higher part of curve and final value at saturation dose must be the same (as this is the characteristic property of material), thus the increase of yield strength must be proportionally smaller.

Model of radiation hardening in Fe-C-Mn type alloys

The changes in stress-strain diagram of tensile test due to radiation hardening can be divided into several steps, differing in the rate of changes of separate parameters. This procedure cannot be based only on the changes of parameters in Petch law (σ_i and k_y) but other parameters, as strength coefficient K and strain hardening exponent n from Ludwig's law ($\sigma = K\varepsilon^n$) must be taken into account. Only then conclusions concerning the form of stress-strain diagram and Lüders strain value can be made. In principle, radiation hardening can be discussed in four stages, as is seen in Fig. 9.

Stage "a" can be observed for very low doses, approximately of 10^{15} to 10^{16} n/cm^2, where local maximum of k_Y with neglecting increase in stress σ_i is caused by irradiation. Only the initial part of diagram is changed, following the increase of Lüders strain value. As the parameter K and exponent n are not changed, post-Lüders parts of diagram are coinciding. Change in defects concentration, induced by irradiation, is negligible to be able to restrict the Lüders strain propagation through the specimen, similarly as atoms, pinning the dislocations, are in the pre - irradiation location.

Stage "b" occurs at neutron doses around 10^{18} n/cm^2, where friction stress is increasing but without any large change in parameter k_Y . As value of strain exponent n is decreasing similarly to the decrease of coefficient K, thus decrease in the slope of diagram and increase in Lüders strain are the results of both processes.

At the doses around 3 to 5×10^{18} n/cm^2 stage "c" appears. This stage is characterized by continued increase in friction stress with simultaneous decrease in parameter k_Y . For these doses parameter K shows small increase but the exponent n is continuously decreasing. As a result the slope of stress-strain curve is almost kept without change, but Lüders strain value begins to decrease. In this dose region the stress necessary for propagation of dislocations through specimen is so high (due to the increase in friction stress as a result of irradiation induced concentration of defects) that slip does not appear only in one group of planes, but starts simultaneously in more groups. This so called "turbulent" slip appears (on the contrary to the unirradiated stage) just after Lüders band propagation has finished.

For doses higher than 5×10^{18} n/cm^2 stage "d" can be observed. In this stage friction stress is still continuously increasing but parameter k_Y strongly falls to zero value. At the same time decrease in exponent n continues and parameter K begins to decrease, too. In consequence of both these changes slope of stress-strain curve is decreasing further. Result of all effects is expressed in the disappearing of Lüders strain and physical yield point. For these doses it is possible to suppose the concentration of obstacles is so high as to suppress free propagation of Lüders strain and this high concentration causes enhanced migration of

carbon and nitrogen atoms out of dislocations (and creating obstacles far from them) so that the yield point can disappear (for doses higher than 1×10^{19} n/cm^2).

All these conclusions are valid especially for pure iron, without any exceptions. For other type of alloys there can be some differences caused by different microstructure and by carbon and manganese presence in alloys.

Conclusions

Results of the radiation damage study (at 80 to 100 C) in binary and ternary Fe-C-Mn type alloys show some effects; the most important ones are :

- radiation damage in this type of alloys results in hardening and embrittlement; hardening is expressed especially by increase of friction stress and yield strength, and by decrease of parameter k_Y . Embrittlement causes elongation decrease and transition temperature increase (based on impact tests)
- radiation damage saturated at doses higher than 10^{19} n/cm^2 and then "supersaturation" region has been observed for several types of alloys, especially for Fe-C- type. "Supersaturation" is characterized by "softening" in strength properties, i.e. by yield strength decrease, without any increase in elongation
- this type of alloys has strong structural sensitivity to radiation damage : structure influence predominates over the free carbon and nitrogen content effect
- for the same type of alloys or steels radiation damage value is dependent on the initial concentration of obstacles, i.e. on the initial yield strength value
- radiation damage value is strongly dependent on the carbon and manganese content in alloys
- influence of carbon content is expressed by the ferrite content in alloys. As the ferrite is the predominantly hardenable phase, with the decrease

of ferrite content in alloys radiation damage is decreased too. Pearlite influences radiation damage value especially in the "supersaturation" region due to softening of phase boundaries

- manganese atoms create complexes with carbon or nitrogen atoms or point defects during irradiation and thus substantially enlarge radiation hardening and embrittlement
- increase of irradiation temperature up to 160 to 180 C causes enlarged hardening in alloys with cca 0.10 to 0.15 % C, because in this temperature range additional hardening by precipitation of ϵ - carbides appears; this process can take place only in the pearlite presence
- on the basis of the changes of individual parameters, found out during tensile tests, model for radiation hardening of Fe-C-Mn type alloys has been proposed.

Acknowledgements

The author is very much indebted to several of his colleagues, whose contributions are gratefully acknowledged. Thanks are also to A.D.Amaev and P.A.Platonov, Institute of Atomic Energy, Moscow; M.Vacek and V.Juřička, Institute of Nuclear Research, Řež near Prague for assistance in carrying out the irradiation and experimental work; to J.Henig and M.Říhová, Škoda Works, for assistance in evaluating the experimental results; and to T.H.Blewitt, Argonne National Laboratory, for helpful discussions and comments.

References

/ 1 / Sekino Shozo, Fujishima Toshiyuki, Trans. Japan Inst. Metals, Vol. 7, No. 2, 1966, p. 142

/ 2 / Cottrell A.H., Trans. Amer, Inst. Min. Metall. Engrs., Vol. 212, 1958, p. 192

/ 3 / Makin M.J., Minter F.J., Mathorpe S.A., Phil.Mag., Vol. 13, 1966, p.729

/ 4 / Blewitt T.H. et al., "Radiation hardening in copper", Int. Conf. on Vacancies and Interstitials in Metals, Jülich, Vol. II, 1968, p.547

/ 5 / de Wit R., Koehler J.S., Phys. Rev., Vol. 116, 1959, p. 1113

/ 6 / Foreman A.J.E., Phil. Mag., Vol. 15, No. 137, 1967, p. 1011

/ 7 / Johnson A.A., Nature, Vol. 189, No. 4767, 1961, p. 826

/ 8 / Beeler J.R., "Computer Studies of neutron irradiation damage and annealing in finite BCC iron specimens", ASTM STP No. 380, p. 86

/ 9 / McRickard S.B., Phil. Mag., 1968, p. 915

/10/ Bement A.L., Dau G.J., Evans E.A., Nightingale R.E., "Reactor Fuels and Materials Development Programs for Fuels and Materials Branch of USAEC Division of Reactor Development and Technology", Quarterly Progress Report, July-Sept. 1968, USAEC Report BNWL-919, Battelle-Northwest, Richland, Nov. 1968

/11/ Bryner J.S., Acta met., Vol. 14, 1969, p. 323

/12/ Baird J.D., Jamieson A., J. Iron Steel Inst., Vol. 204, 1966, p. 793

/13/ Damask A.C., "Effects of neutron irradiation on precipitaion of carbon in alpha-iron", Int. Conf. on Diffusion in B.C.C. Materials, 16-18.9.1964, Technical Report BNL-8418

/14/ Rossi F.S., Castagne M., Ferro A., Sébille J., "On the effect of nitrogen on the mechanical properties of neutron irradiated pure iron".
Symp. on the Effects of Radiation on Structural Metals, Atlantic City, June 29-July 1, 1966
Technical Report SORIN 87, 1966

Tab. 1. Composition of the experimental alloys

Alloy	C	Mn	Si	P	S	Cr	Ni	Mo	Cu
	Analysis, wt. per cent								
XP - Fe	0,02	-	0,08	0,001	0,010	0,03	0,04	0	-
XB - Fe-0,15 C	0,15	0,08	0,02	0,018	0,028	0,08	0,04	0	0,08
XC - Fe-0,25 C	0,27	0,10	0,05	0,002	0,009	0,03	0,04	0	-
XD - Fe-0,40 C	0,39	0,07	0,05	0,005	0,012	0,03	0,03	0	-
XE - Fe-0,3 Mn	0,01	0,28	0,01	0,002	0,010	0,03	0,03	0	-
XH - Fe-1,0 Mn	0,01	1,05	0,02	0,006	0,025	0,03	0,05	0	0,06
XI - Fe-1,25 Mn	0,01	1,27	0,01	0,003	0,010	0,03	0,04	0	-
XO - Fe-0,1 C - 0,3 Mn	0,08	0,27	0,07	0,002	0,016	0,04	0,07	0	0,08
XX - Fe-0,1 C - 0,7 Mn	0,12	0,66	0,01	0,003	0,011	0,04	0,05	0	-
XS - Fe-0,1 C - 1,2 Mn	0,06	1,25	0,01	0,011	0,024	0,03	0,05	0	0,07
XL - Fe-0,2 C - 0,8 Mn	0,20	0,85	0,01	0,001	0,010	0,05	0,05	0	0,01
XM - Fe-0,3 C - 1,8 Mn	0,34	1,83	0,04	0,002	0,010	0,03	0,05	0	0,01

Tab. 2. Properties of the experimental alloys at room temperature

Alloy	Lower Yield Strength kg/mm^2	Ultimate Tensile Strength kg/mm^2	Elongation 10 x D %	Friction Stress kg/mm^2	k_Y C.G.S.u.	Transition Temperature (Impact) deg C
XP - Fe	14.3	26.8	34.2	8,2	$1,6x10^7$	- 48
XB - Fe-0,15 C	27.0	37.6	31.7	16.3	1.4	+ 12
XC - Fe-0,25 C	17.9	39.7	28.6	16.7	0.3	+ 33
XD - Fe-0,40 C	21,0	43.7	24.2	18,0	-	+ 62
XE - Fe-0,3 Mn	17.3	27.2	33.2	12.5	1.1	+ 72
XH - Fe-1,0 Mn	16.5	31,0	31,0	12.6	1,0	- 50
XI - Fe-1,25 Mn	19,2	33.3	30.4	12,5	1.4	- 40
XO - Fe-0,1C-0,3Mn	20,4	33.6	31,3	14,3	1,0	-
XX - Fe-0,1C-0,7Mn	19.5	35.1	32,0	11,9	1.4	- 24
XS - Fe-0,1C-1,2Mn	22.6	37.2	29.0	14.3	1.4	- 48
XL - Fe-0,2C-0,8Mn	22.8	40.8	27.1	19.7	0.6	- 25
XM - Fe-0,3C-1,8Mn	$39,6^x$	69.4	15.4	-	-	+ 12

x - 0,2 % offset yield strength

Tab. 3. Composition and properties of ČSN 13030,9 Ni, Al + Ti steel

Chemical analysis, wt. per cent

C	Mn	Si	P	S	Cu	Cr	Co	Ni	Ti	Al
max 0,20	1,1- 1,4	0,20- 0,40	max 0,020	max 0,020	max 0,15	max 0,20	max 0,010	0,30- 0,45	0,02- 0,05	0,02- 0,05

Room temperature mechanical properties

Yield Strength kg/mm^2	Ultimate Tensile Strength kg/mm^2	Elongation 5 x D %	Reduction of Area %
min 22	min 44	min 22	min 45

List of figures

Fig. 9. Changes in stress-strain curves for iron irradiated to various neutron doses as a result of radiation hardening.

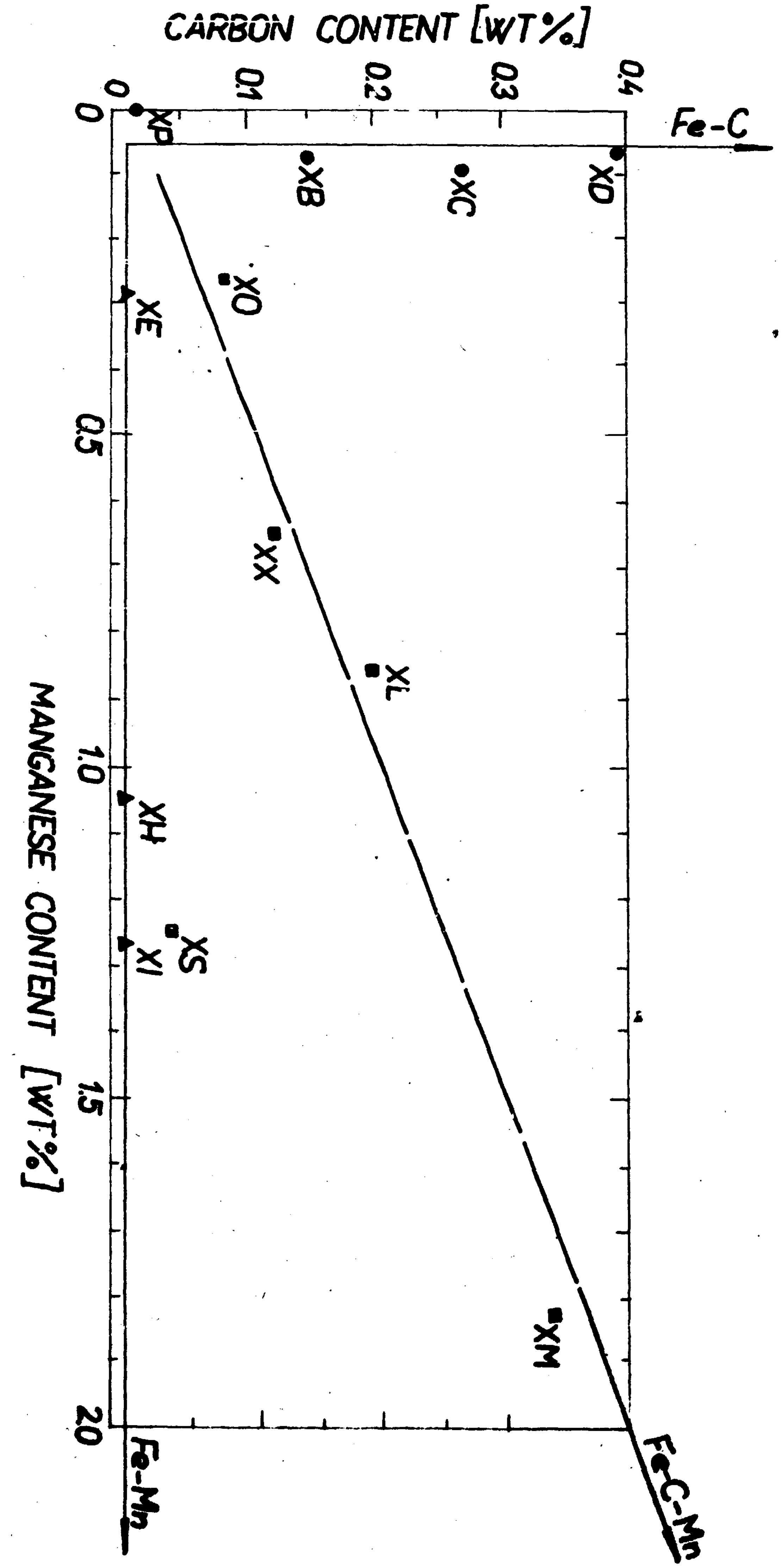

FIG. 1

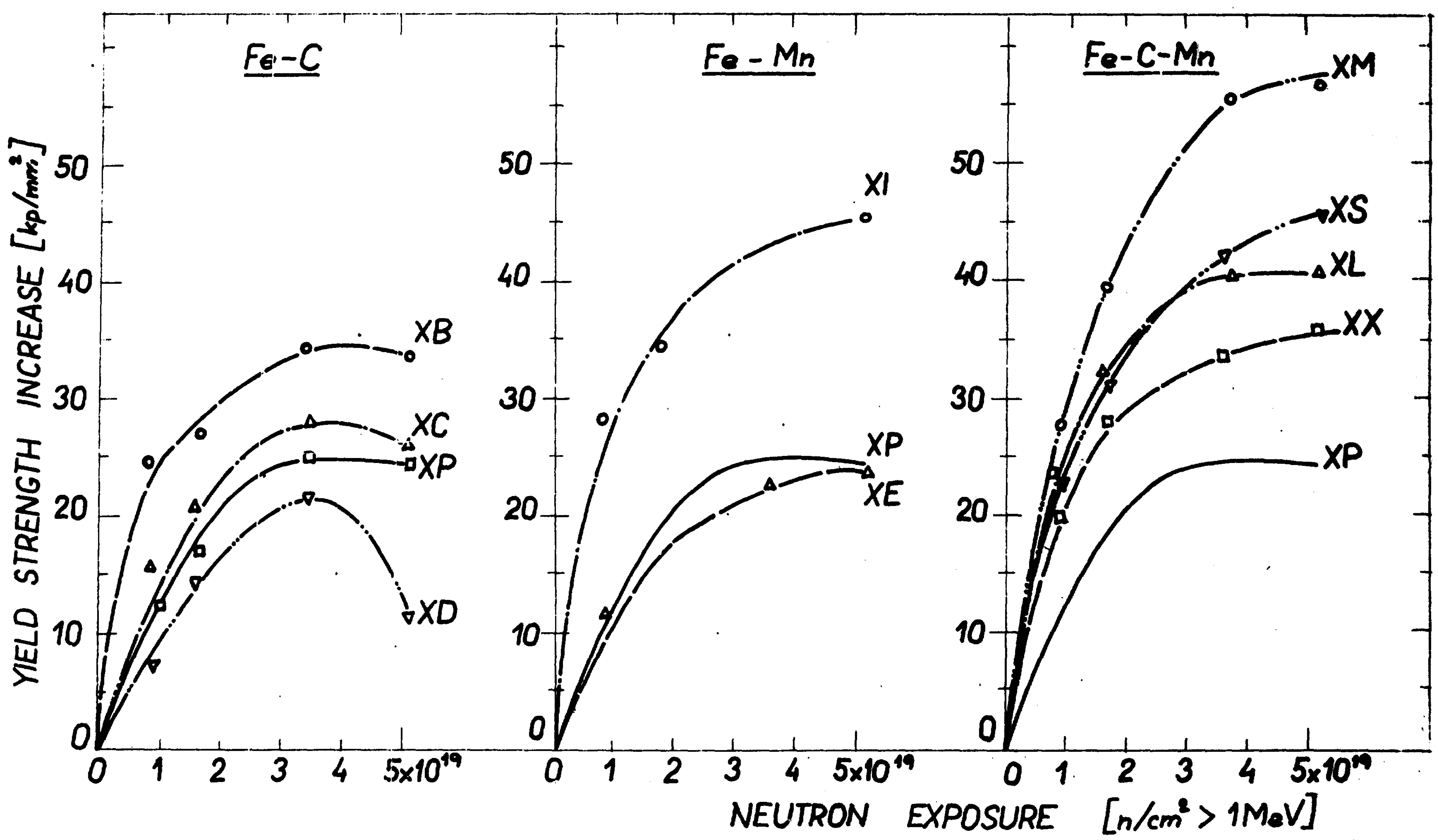
Fe-C
Fe - Mn
Fe-C-Mn
YIELD STRENGTH INCREASE [kp/mm²]
XB
XC
XP
XD
XI
XP
XE
XM
XS
XL
XX
XP
NEUTRON EXPOSURE [n/cm² > 1MeV]

FIG. 3

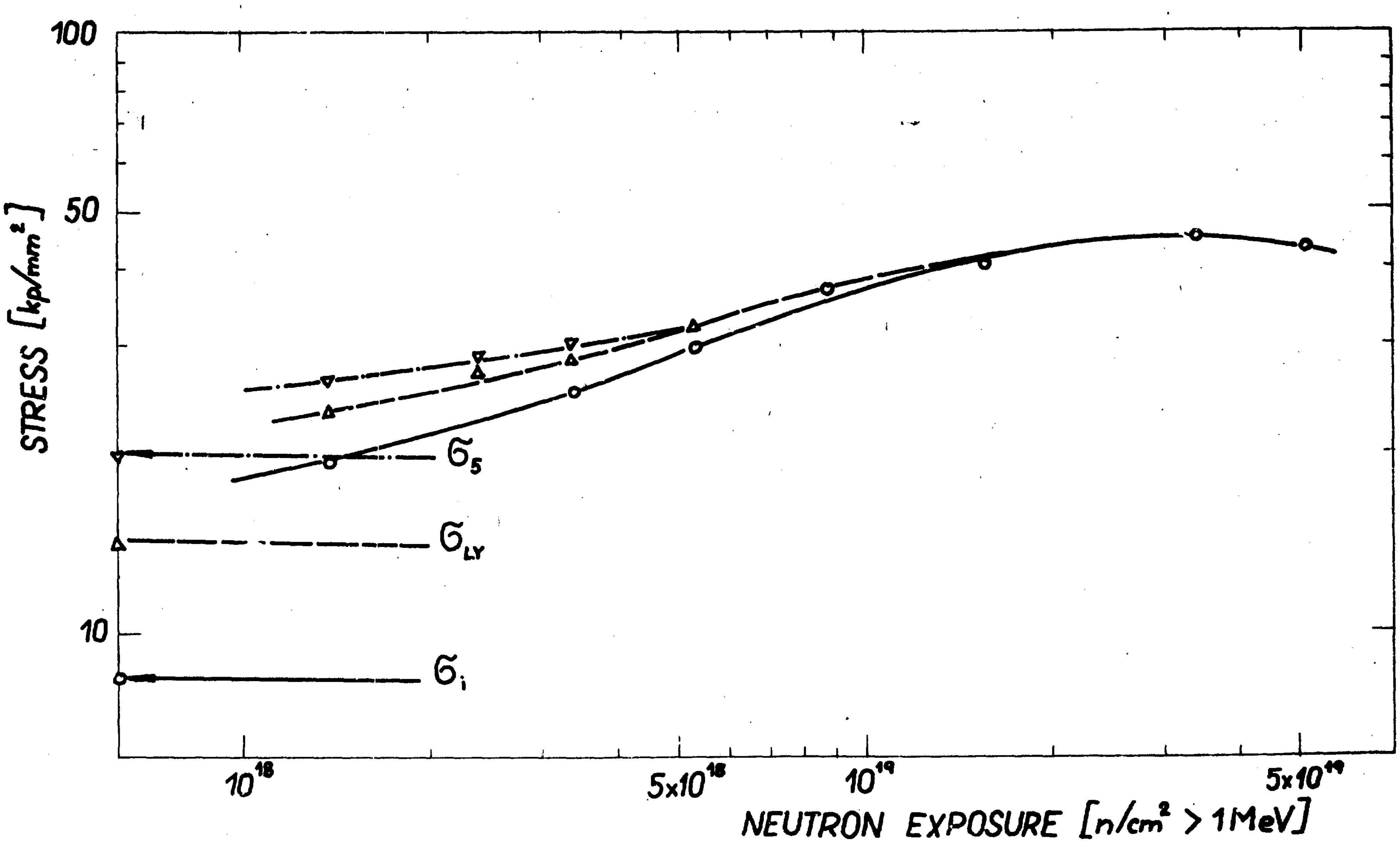
STRESS [kp/mm²]
σ5
σLY
σi
NEUTRON EXPOSURE [n/cm² > 1MeV]

FIG. 2

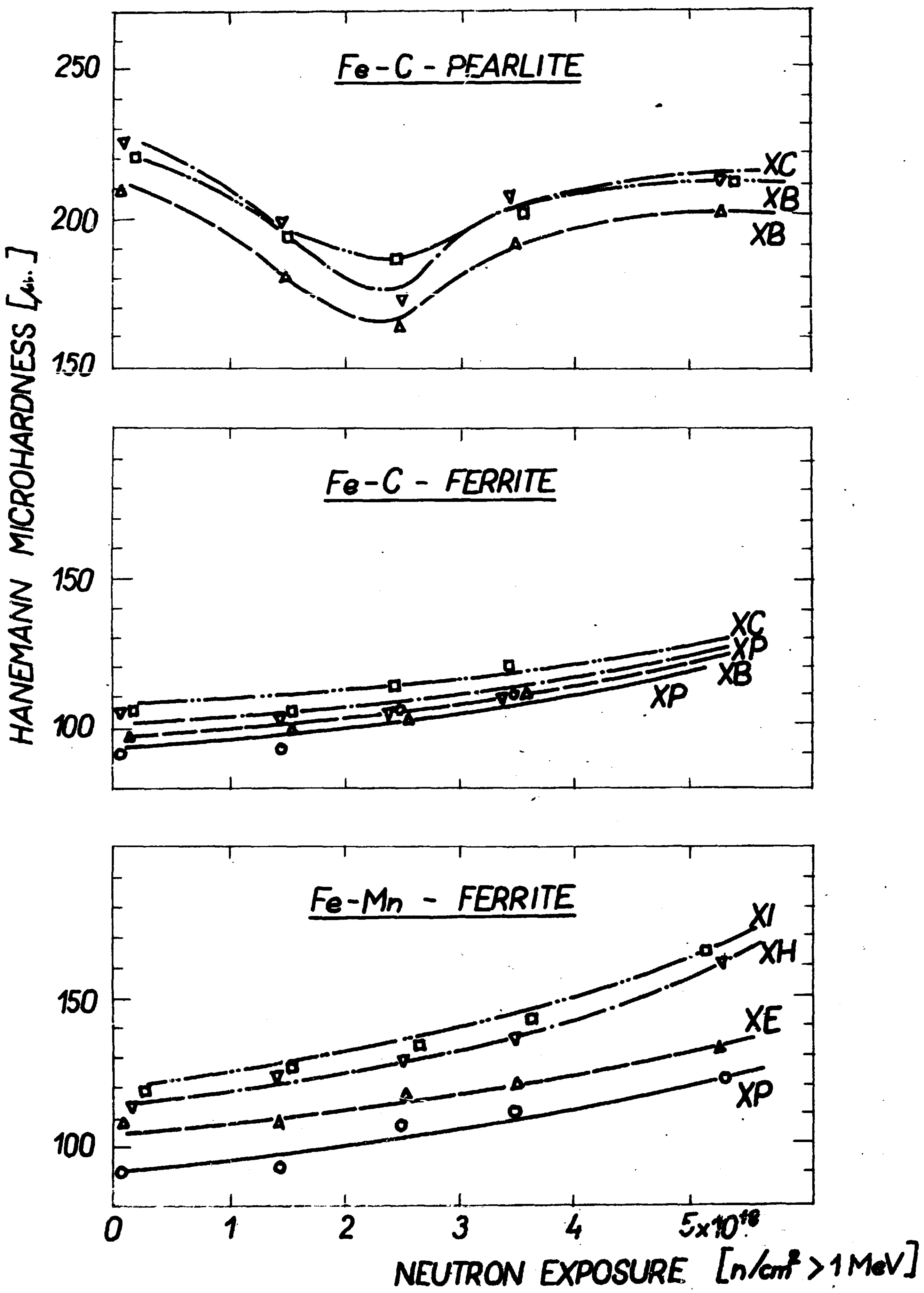

Fe-C - PEARLITE
XC
XB
XB
Fe-C - FERRITE
XC
XP
XB
XP
Fe-Mn - FERRITE
XI
XH
XE
XP
HANEMANN MICROHARDNESS
NEUTRON EXPOSURE [n/cm² > 1 MeV]

FIG. 4

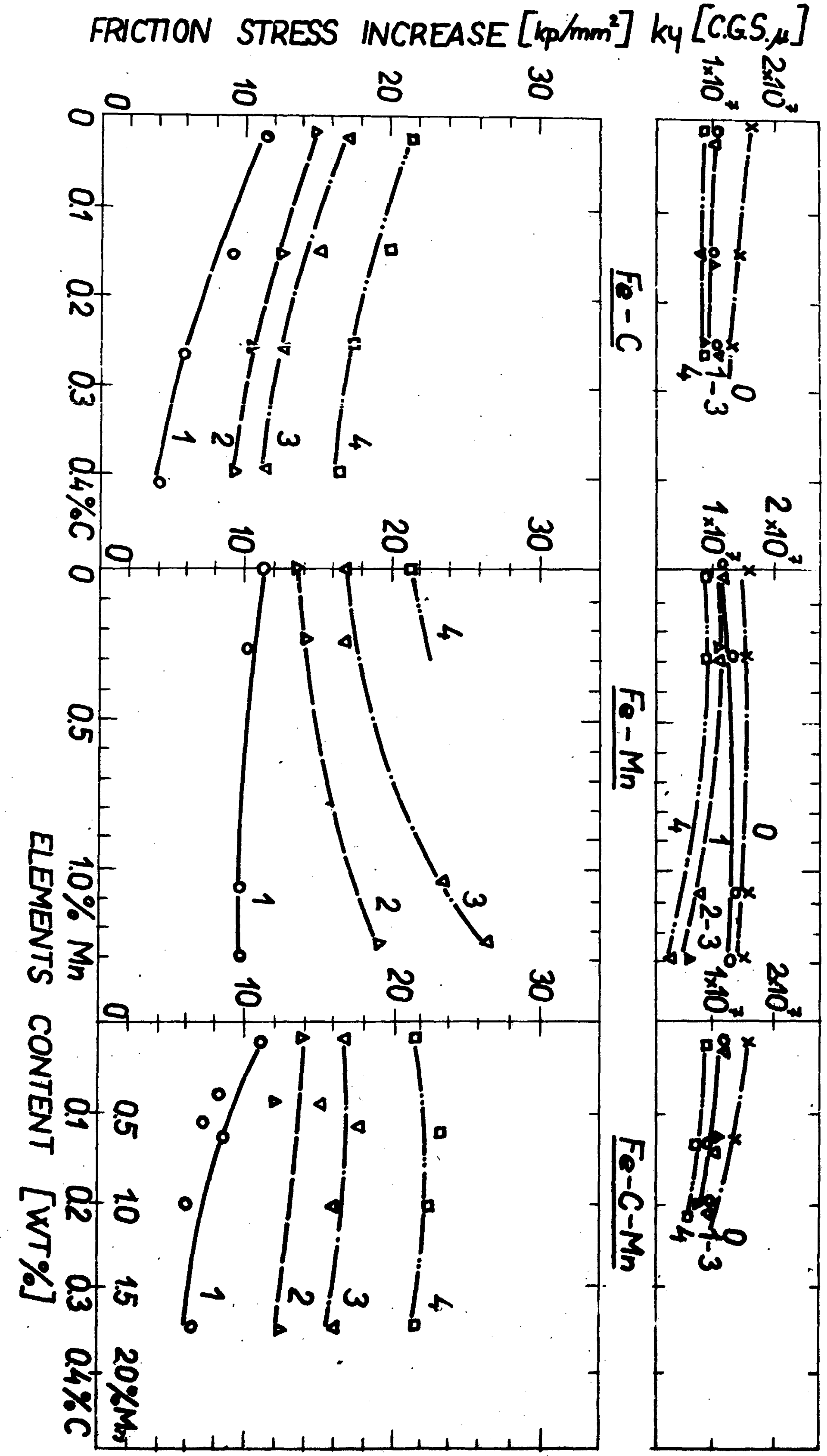

FRICTION STRESS INCREASE [kp/mm²]
Fe-C
Fe-Mn
Fe-C-Mn
ELEMENTS CONTENT [WT%]

FIG. 5

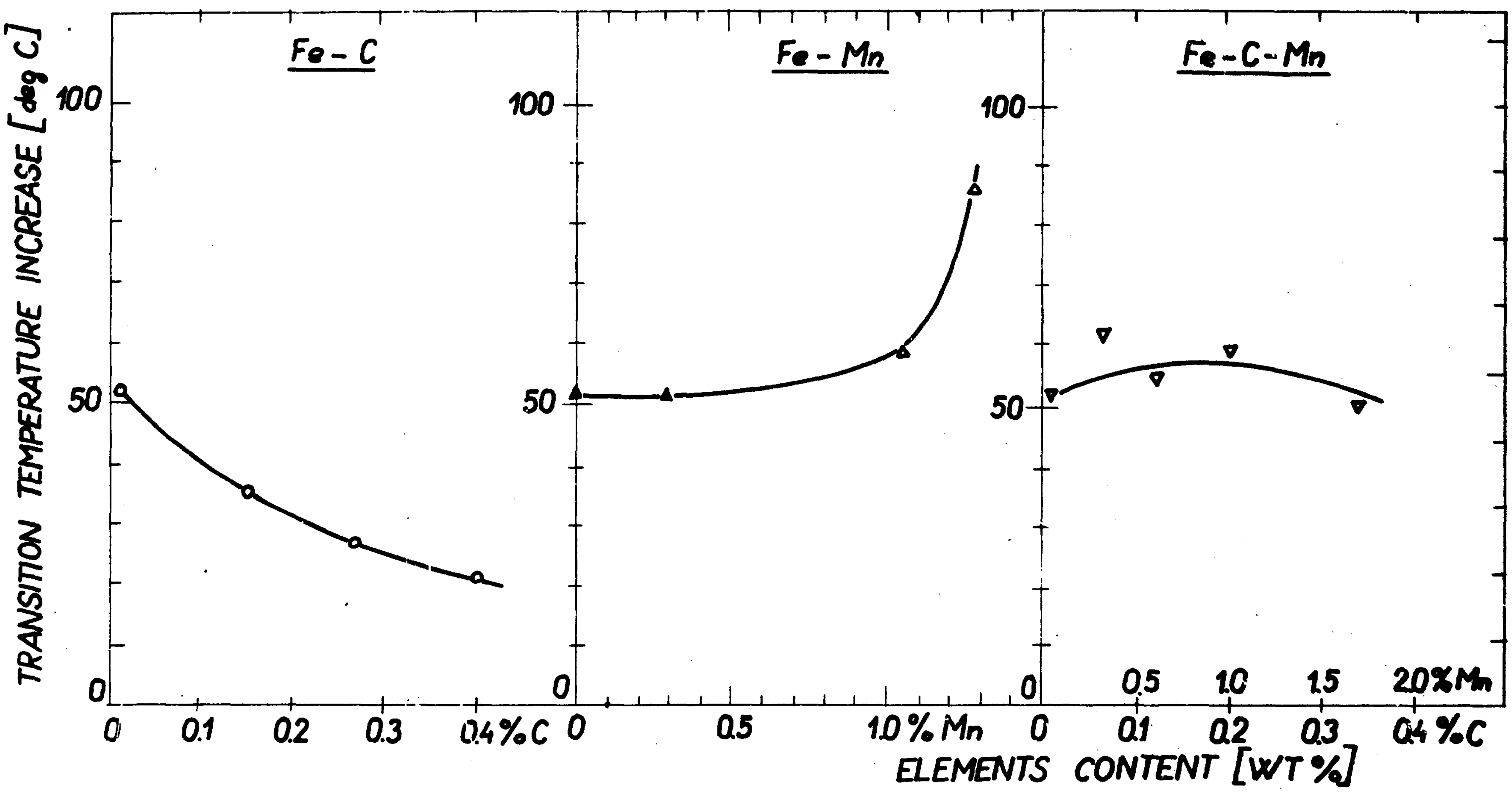

TRANSITION TEMPERATURE INCREASE [deg C]
Fe - C
Fe - Mn
Fe - C - Mn
100
50
0
0.1
0.2
0.3
0.4 % C
0.5
1.0 % Mn
1.5
2.0 % Mn
ELEMENTS CONTENT [WT %]

FIG. 7

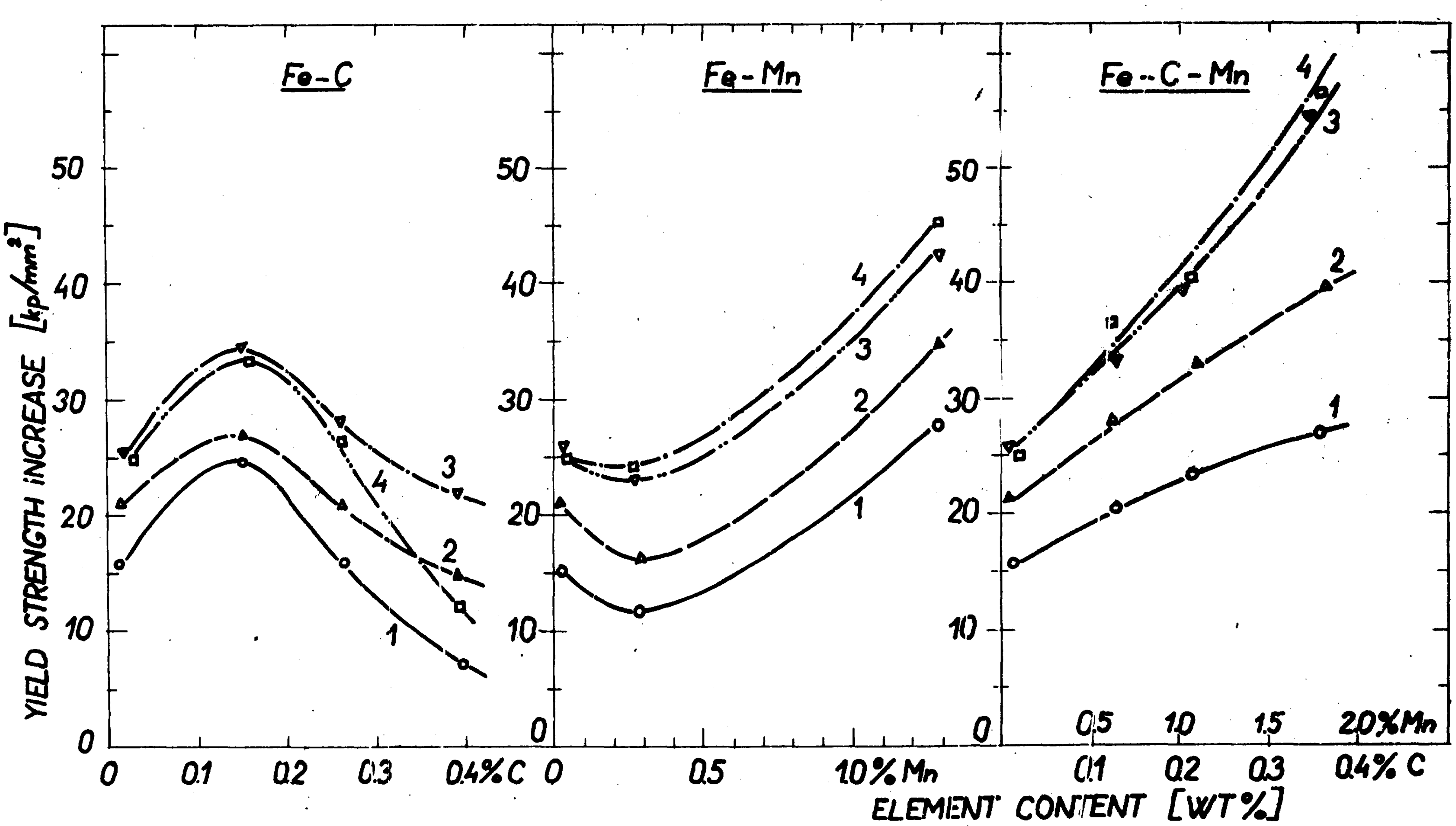

YIELD STRENGTH INCREASE [kp/mm²]
Fe - C
Fe - Mn
Fe - C - Mn
50
40
30
20
10
0
1
2
3
4
0.1
0.2
0.3
0.4 % C
0.5
1.0 % Mn
1.5
2.0 % Mn
ELEMENT CONTENT [WT %]

FIG. 6

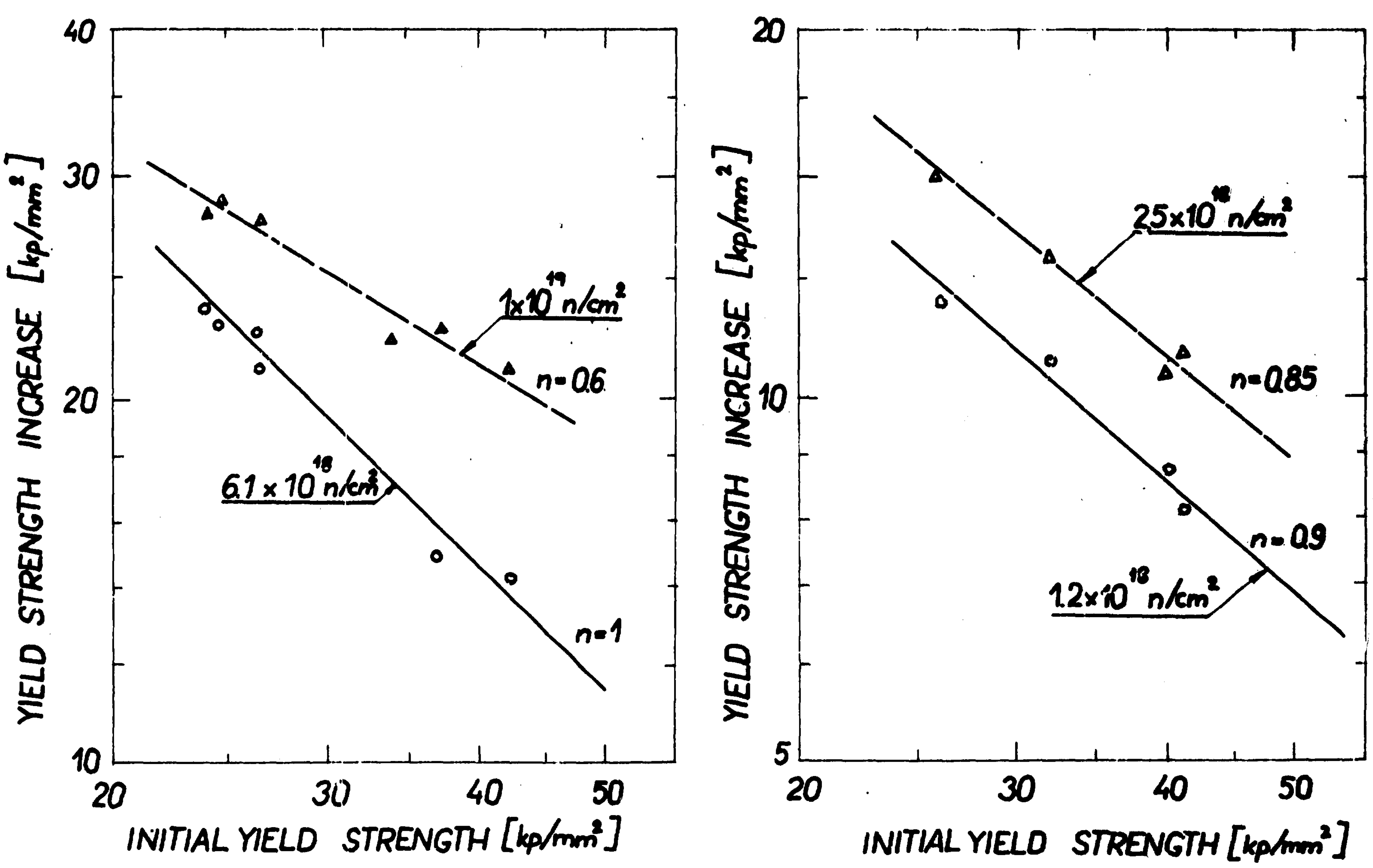
YIELD STRENGTH INCREASE [kp/mm²]
INITIAL YIELD STRENGTH [kp/mm²]
1×10¹⁹ n/cm²
n=0.6
6.1×10¹⁸ n/cm²
n=1
2.5×10¹⁸ n/cm²
n=0.85
n=0.9
1.2×10¹⁸ n/cm²

FIG. 8

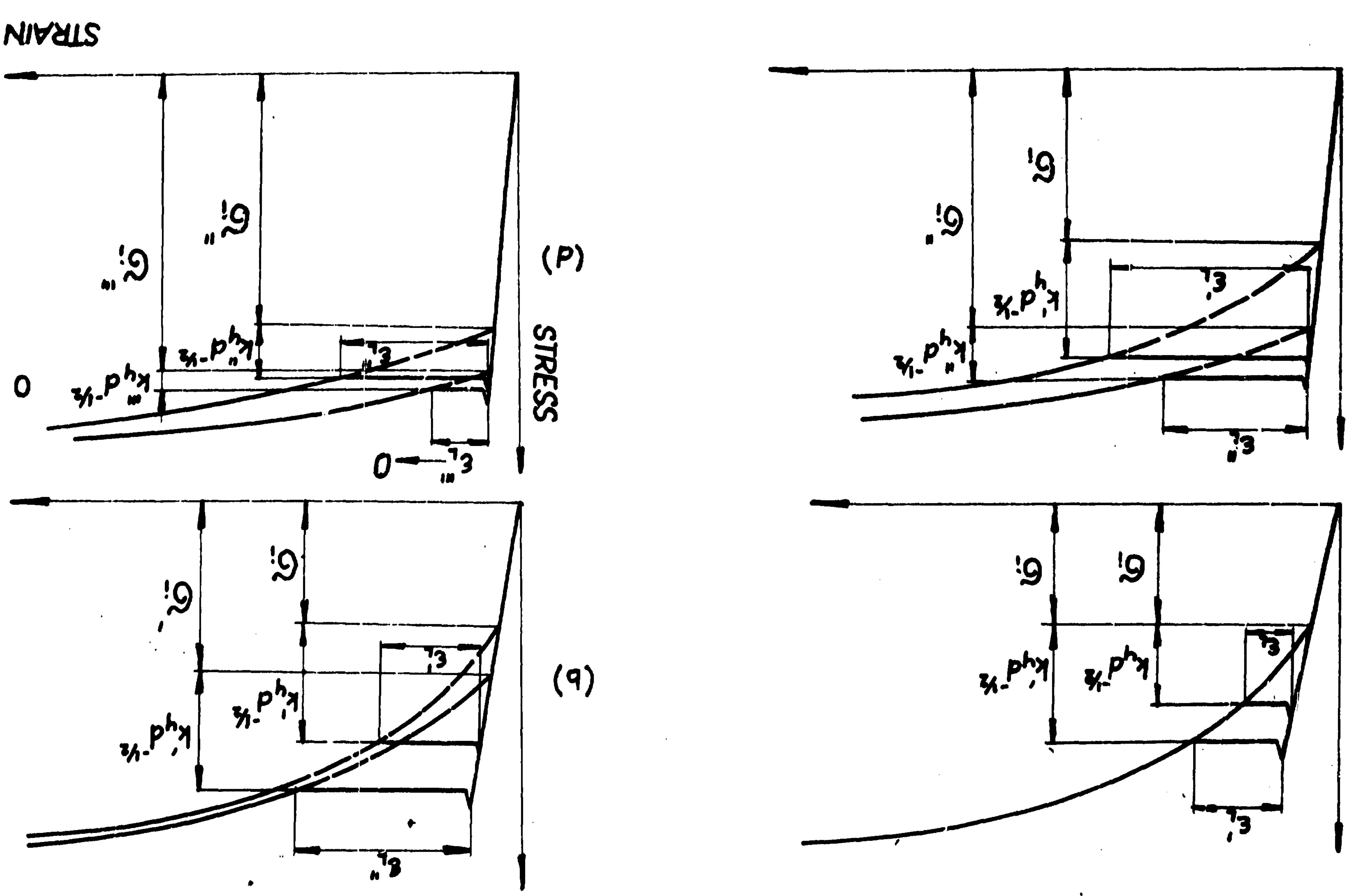
STRAIN
STRESS
(a)
(b)
(c)
(d)

FIG. 9